ADVANCE OF THE CONTACT LINE OF A LIQUID-AIR FRONT IN A MICROCHANNEL FOR DIFFERENT GEOMETRIES

Author: Emma Oriol Ferrero
*Facultat de Física, Universitat de Barcelona, Diagonal 645, 08028 Barcelona, Spain.**

Advisor: Aurora Hernández-Machado and Pamela Vazquez-Vergara

Abstract: The aim of this work is to study the fluid-front dynamics within microchannels of different geometries. A first rectangular and hydrophobic microchannel has a groove geometry reproducing a defect. A second geometry consists in many wedges repeated along an hydrophilic microchannel. The latter has a specific geometry that together with the hydrophilic contact angle causes a mass injection that partially compensates friction.

I. INTRODUCTION

Microfluidics is an increasingly important field which allows the study of complex fluids such as blood. Applications are mainly focused in diagnostic, since only a small amount of liquid is required. Furthermore, the dynamic study is necessary because the particles of these fluids might deform, orientate, change their membrane properties, etc.[1]

Nevertheless, imperfections during fabrication are unavoidable and at this scale, they might become relevant. Pinning of the contact line is an important effect: when the front reaches a sharp structure, it gets pinned on one side and slowed down. Then it is followed by an avalanche. In a groove geometry the Fakir state can be observed, i.e., the fluid does not enter the groove.

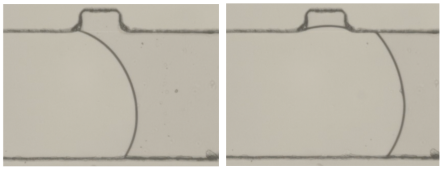

FIG. 1: Left: pinning of the contact line in a groove corner. Right: the front recovers the advance after attaching to the other corner of the groove. The fakir state is observed.

It is refered as spontaneous imbibition, when a fluid enters a porous medium without an additional force. This happens, e.g., when a water droplet expands trough paper. On the other hand, forced imbibition requires an external force that compels the fluid to enter the medium, as could be an hydrophobic microchannel. This can be achieved with the use of a pump or by hydrostatic pressure.

This work aims to study two cases. First, an hydrophobic microchannel which is used to study the pinning mechanism of the contact line during forced imbibition. It has a small groove that recreates a small defect. In this case, the pressure forcing the front to advance is hydrostatic. Besides, we study a hydrophilic channel with many wedges repeated along its length. Here, the only driving force is the capillary pressure gradient. Furthermore, the specific patterns endeavor to oppose the friction slowing down the interface and to achieve a linear regime. The physics responsible for this neutralizing is a Young-Laplace balance leading to a mass injection. At the edge of the wedge, the front presents an hydrophobic dynamic angle. However, the hydrophilic angle should be recovered and the front would rapidly climb the vertical wall in order to do so. The study is focused in one wedge.

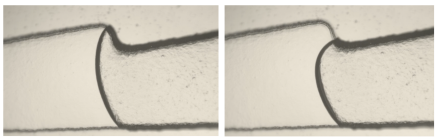

FIG. 2: Left: the front at the edge presents a dynamic hydrophobic angle. Right: the front recovers the dynamic hydrophilic angle climbing the vertical wall.

The work consists in studying the behaviour of the water-air contact line as a function of time and other aspects as the velocity of the front. The advance of the front is analyzed for two different geometries, one of them presenting a pinning mechanism, the other presenting a mass injection that partly compensates dissipation.

II. THEORETICAL MODEL

The equations describing the flow through a channel depend on the channel dimensions and structure. Here, we deduce the governing equations for a rectangular channel and for a wedge. In both cases, since the channel width is bigger than the channel height ($w >> b$), a two-dimensional flow can be considered. Besides, low Reynolds number can be considered at this scale and velocity.

The mean front position, $h(t)$ is obtained as the mean of the positions for each pixel along the width of the

*Electronic address: emma.orfe@gmail.com

channel, i.e.,

$$h(t) = \frac{1}{N}\sum_{i=1}^{N} h_i(t) \tag{1}$$

where $h_i(t)$ is the distance travelled by the contact line for one point, i, and i goes over the pixels on the width of the channel.

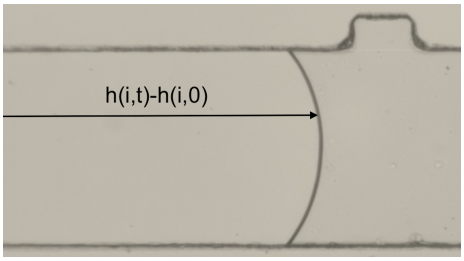

FIG. 3: The distance of the arrow coincides with the front position at the i^{th} pixel of the contact line. The offset $h_i(0) = h(i,0)$ is the distance already travelled by the front that cannot be seen in the microscope.

From the Navier Stokes equation we derive the following equation. The equation is simplified considering a low Reynolds regime and a two-dimensional flow [2].

$$\frac{d}{dt}(h\dot{h}) + \frac{12\eta}{\rho b^2}h\dot{h} = \frac{\Delta P}{\rho} \tag{2}$$

where h is the mean front position, $\dot{h}$ the mean front velocity, ρ and η are the fluid density and viscosity, respectively, b is the height of the channel and ΔP is the contribution of all pressures. The term $A = \frac{\Delta P}{\rho}$ is related with the advance forces and the term $\frac{12\eta}{\rho b^2}h\dot{h}$ with dissipation.

We first consider the case of a rectangular hydrophobic channel. In this case $\Delta P = P_{hyd} - P_L$. The front advances due to a hydrostatic pressure, P_{hyd}, while the Laplace pressure (capillary pressure), P_L, is opposed to the advance. The hydrostatic pressure is achieved by a container full of fluid that is connected to the channel through a tube. It has to be taken into consideration that the tube opposes a resistance. The previous equation results in [3]

$$\dot{h}(t) = \frac{P_{hyd} - P_L}{\eta\left(\frac{12h(t)}{b^2} + \frac{8bwl_t}{\pi r^4}\right)} \tag{3}$$

where w is the width of the channel, l_t is the tube length and r is the tube internal radius.

This equation is linear at small times and follows the Washburn regime ($h \sim t^{1/2}$) for longer times. For a tube of a considerable length the resistance is big enough to consider the velocity constant along the microchannel [3].

Consider now the hydrophilic channel with a wedge geometry. In this case $A = \frac{P_L}{\rho}$ since the capillary pressure is the only propelling force. Equation 2 can be integrated for a wedge geometry and the exponent obtained for long enough times is 1/3 since geometry is not constant [4].

This would happen for a channel with one wedge geometry. Our case concerns a repetition of wedges. In this case, when the contact line arrives at the wedge superior edge, the dynamic contact angle is hydrophobic since it is bigger than $\pi/2$ rad. However, the contact line must recover its dynamic hydrophilic angle. This balance happens very fast and as a consequence there is a mass injection to the front. This mass injection might partly compensate dissipation. If this happened, a linear regime over a finite number of wedges would be achieved [5].

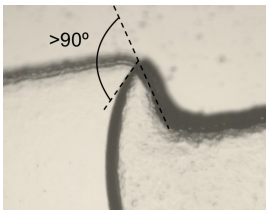

FIG. 4: The dynamic contact angle with the vertical wall is hydrophobic.

III. MATERIALS AND METHODS

A. Microchannel fabrication

The entire fabrication process is done in the Clean Room of the Physics Faculty of UB.

During this work, two microchannels have been used. One of them is hydrophobic with one groove simulating a small imperfection (A). The other is hydrophilic with many wedges repeated through the channel (B). Both of them are hydrophobic without treatment however experiments are only done under hydrophilic conditions for channel B.

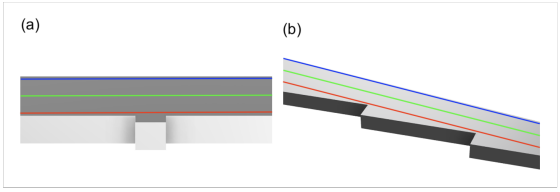

FIG. 5: (a) Rectangular microchannel with a groove geometry (A). (b) Microchannel with a rectangular cross section and repeated wedge geometry (B). The red line indicates the "top" point, the green line the "center" point and the blue line the "bottom" point.

The process to obtain a microchannel has been the following. Firstly, the mold has been designed with both

Autodesk Fusion and *Preform* software. Hereafter, the mold is 3d-printed and then rinsed with isopropyl alcohol.

Once the mold is dry, the organic polymer polydimethylsiloxane (PDMS) is poured onto the mold and put into the oven in order to achieve polymerization.

Then, the hardened polymer is removed from the mold and is put through a first oxidation process, together with a cleaned glass slide. The oxidation process consists in having both pieces inside a vacuum chamber (Harrick Plasma Cleaner) at low pressures filled with O_2 . Then a high frequency voltage is applied in order to obtain the plasma. The polymer and the glass are exposed to the plasma for 60 seconds. This process activates the PDMS (and the glass microscope slides) and polar functional groups appear on the surfaces. When both materials are in contact, they are strongly bonded [6].

TABLE I: Microchannel dimensions. Width (w), height (b) and length (l) of the channel as well as the length of the geometry (l_g) are presented.

	Microchannel A	Microchannel B
w_{min} (μm)	300	700
w_{max} (μm)	350	1000
b (μm)	100	300
l_g (μm)	100	2000
l (cm)	4	5.4

B. Hydrophilic treatment for a microchannel

In order to achieve a hydrophilic surface, the microchannel undergoes another oxidation process, longer this time. The bonding process and the hydrophilic treatment must be done separately, since the bonding of the PDMS to the glass is hindered by long oxidation processes. This time the exposure to plasma lasts 500 seconds. Afterwards, the channel has hydrophilic properties and it is ready for the experiments.

Once activation is finished, PDMS starts a process named hydrophobic recovery. This recovery is attributed to different processes (diffusion, redistribution of radicals between the surface and the bulk...) that reduce the energy of the system and that are widely affected by temperature and contamination [7]. This means that the hydrophilic behaviour of the channel is temporary and the contact angle will vary with time.

C. Experimental method

The set up of the experiment differs for spontaneous imbibition or forced imbibition. In both cases, an optical microscope Optika B350 with a 4X and 10X magnification is used. The microscope is connected to a Chronos 1.4 High Speed Camera. The experiments were recorded from 700 to 7000 frames per second. The fluid used for the experiments is Milli-Q® water, which is a well-known newtonian fluid.

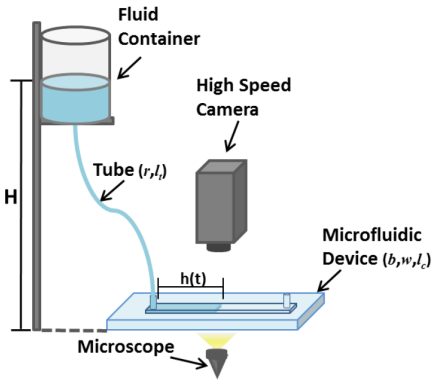

FIG. 6: Schematic experimental set up for forced imbibition. (C. Trejo 2016)

For the forced imbibition, the microchannel is connected to a fluid container using a tube. This container is big enough to consider that its height will not change and the hydrostatic pressure will be constant (Fig. 6). Spontaneous imbibition does not require any external force. The fluid was introduced in the inlet reservoir using a micropipette.

D. Data processing

The image processing has been done with a MATLAB program. The program worked subtracting to every image the previous one [8] and then applying filters to finally obtain the contact line for every time step. For high frame rates, information was being repeated and the front contact line was lost. In order to solve this, the subtracted image was the n^{th} previous image, i.e., the image 35 was subtracted to the image 35+n, were n was ranging from 10 to 30.

The program calculates the mean front position using Equation 1 and tracks the position of three specific points of the contact line (Fig. 5). The time derivative of $(h - h_0)$ and the time derivative of $(h - h_0)^2$ are calculated as well as a numerical derivative, following the equation

$$\frac{\Delta h}{\Delta t} = \frac{h(i+n) - h(i)}{n \cdot \Delta t} \tag{4}$$

where $\Delta t = F^{-1}$, F being the frame rate, $h(j)$ is the front position in the j^{th} time step for $j = i, i+n$. The equation is used for $n = 1$. Nevertheless, for videos with higher frame rate n is increased. The derivative of $(h - h_0)^2$ is calculated changing $h(j)$ by $h(j)^2$.

Finally, assuming the front advance pursues an equation such as

$$h(t) - h_0 = v_0 \cdot t^{\nu} \tag{5}$$

which can be linearized applying logarithms on both sides, the program calculates ν for a window of points. This window is chosen manually assuring enough points are used for the regression. This window value induces an error of $\delta\nu = \pm 0.2$.

IV. RESULTS AND DISCUSSION

A. Hydrophobic channels

The front is slowed down by the pinning and then its velocity increases to recover the linear behaviour. This can be observed in Fig. 7. The exponent ν for the "top" point has a depression followed by a jump, from $\nu = 0.5 \pm 0.2$ to $\nu = 2.0 \pm 0.2$. This can be compared with the velocity in Fig. 8. There is a jump in the velocity at the same time the front arrives to the other corner of the groove. There are small pinning mechanisms during the front advance that present lower exponents and are covered by the global front advance. In Fig. 8 it can be observed the front velocity and the derivative of h^2. The exponent obtained for the mean front position $(h(t) - h_0) \sim t^{\nu}$ is $\nu = 0.96$. The velocity should present $\nu - 1 = -0.04$ and $dh^2/dt \sim t^{2\nu-1}$ such that $\nu = 0.92$ which agree with the values presented.

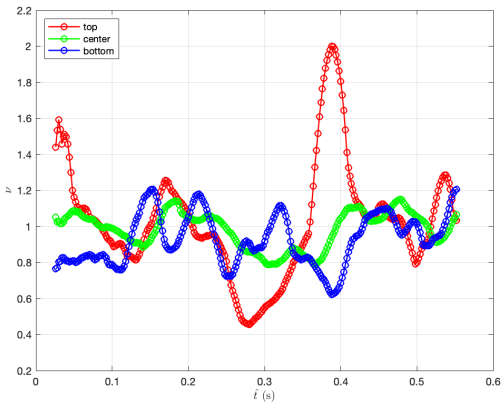

FIG. 7: Exponent ν as a function of time $\hat{t}$ for three points of the contact line. The time is the mean value over the window chosen. The results correspond to microchannel A.

B. Hydrophilic channels

For the hydrophilic channel it can be observed in Fig. 9 the front advance in three different positions. In the "top" position two jumps can be observed. A first with a $\nu = 1.96$ exponent and a second one with a lower exponent of $\nu = 1.76$. This can be observed in Fig. 10. Besides, there is a reply of the bottom part of the contact line (as well as the center) with a certain phase difference.

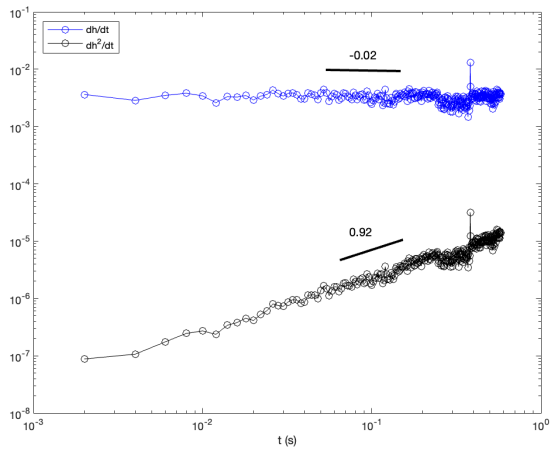

FIG. 8: Representation of the time derivative from the mean front position, dh/dt, and the second power of the mean front position, dh^2/dt as a function of time for microchannel A[9].

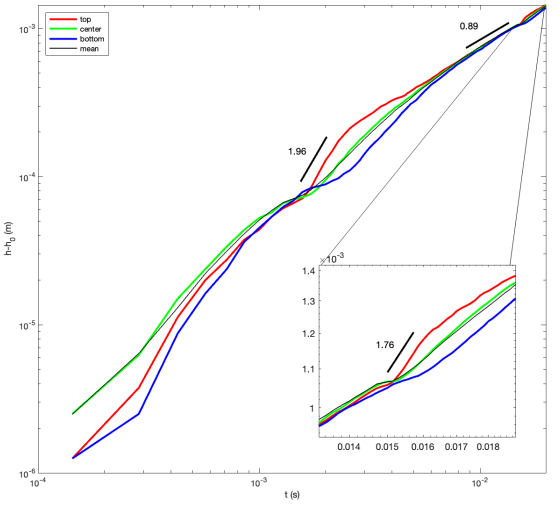

FIG. 9: Mean front position $(h - h_0)$ in meters as a function of time in seconds for microchannel B. The behaviour for three different points is represented as well. The numbers presented in black represent the exponent ν in Eq. 5.

After the first wedge wall is climbed, the front presents a behaviour of the mean front with $\nu = 0.89$ (Fig. 9). In Fig. 10 the exponents fluctuate around this value.

These jumps can also be observed in the velocity (Fig. 11) which is slowed down before increasing again. This can be observed in the video: when the contact line is travelling the vertical wall of the wedge, the bottom part of the front is slowed down and, since the fluid is being injected from the top, the curvature of the contact line is increased. Thereafter, the front recovers the dynamic contact angle and an increase in velocity is observed.

It is noticeable the high values of the velocity. This

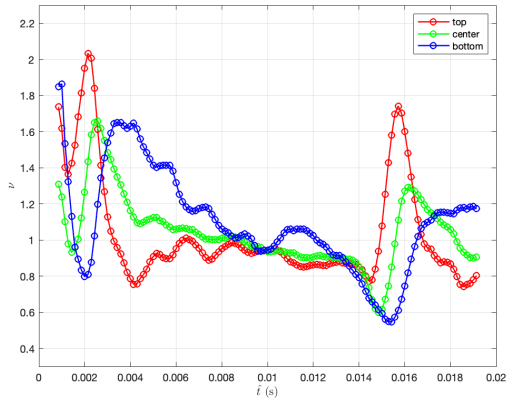

FIG. 10: Exponent ν as a function of time $\hat{t}$ for three different points of the contact line. Red for the top point, green fro the center point and blue for the bottom point. The time is the mean value over the window chosen. The results correspond to microchannel B.

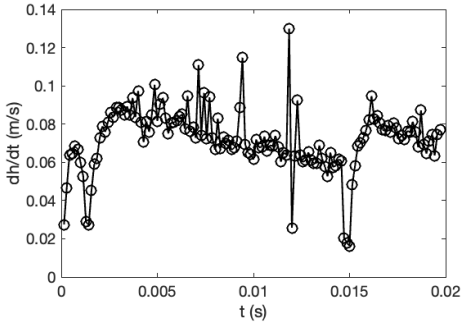

FIG. 11: Time derivative of the mean front position as a function of time for microchannel B. Velocity is decreasing slowly, then it falls down before jumping and repeating the process.

velocity is rapidly reduced in the first wedges. It can be observed that after the rapid increase, the velocity recovers a lower value than in the previous wedge wall.

V. CONCLUSIONS

We have studied the contact line advance for a water-air front in microchannels that have different geometries: a groove and a repetition of wedges.

For the hydrophobic microchannel with the groove, it is verified that the front has a general linear regime ($t^{0.96}$). However when the first pinning occurs the front is slowed down considerably. This is followed by the attachment to the other corner of the groove and an avalanche. This mechanism affects the global dynamics during the time between the pinning and slightly after the attachment to the second corner.

For the hydrophilic microchannel with the repeated wedge geometry it is observed that the front does not recover the same conditions when it starts a new wedge. This is in agreement with the theory, since mass injection only compensates friction partially. It is observed how the front presents a rapid increase in its velocity in the closest part to the wedge (top), while it is slowed down in the opposite side (bottom) just to increase it again afterwards. This rapid increase occurs when the front recovers the hydrophilic contact angle at the vertical wall and there is a mass injection as a consequence. Besides, the velocity of the front is considerable and it is reduced rapidly. Further studies should be made in order to study the behaviour in more than one wedge.

Acknowledgments

I would like to thank both my advisors. Aurora Hernández-Machado for her time, trust and advise as well as Pamela Vazquez-Vergara for her endless help and generosity. I would also like to thank my laboratory colleagues, Óscar Castillo and Andreu Benavent, for their help and insightful conversations, and Lourdes Mendez for her help during fabrication. I could not forget to thank my family and friends for their love and support.

[1] G.B. Thurston. Viscoelasticity of Human Blood. *Biophysical Journal*, 1972, 12, 9.

[2] M. Pradas Gené *Interfaces in disordered media.* Ph.D. thesis, University of Barcelona, 2009.

[3] C. Trejo Soto. *Front Microrheology of biological fluids.* Ph.D. thesis, University of Barcelona, 2016.

[4] M. Reyssat, L. Courbin, E. Reyssat and Howard A. Stone. Imbibition in geometries with axial variations. *Journal of Fluid Mechanics* 2008, 615.

[5] I. domínguez-Román, Rafael A. Barrio and A. Hernández-Machado. Fluid front advance in hydrophilic structured microchannels. Preprint.

[6] A. Borók, K. Laboda and A. Bonyár. PDMS Bonding Technologies for Microfluidic Applications: A Review. *Biosensors* 2021, 11, 8.

[7] B. Jalal, H. Hamidou, K. Philippe, V. Marie-France and R. Vincent. Singularities in hydrophobic recovery of plasma treated polydimethylsiloxane surfaces under non-contaminant atmosphere. *Sensors and Actuators A: Physical* 2013, 197.

[8] V. Heiskanen, K. Marjanen and P. Kallio. Machine Vision Based Measurement of Dynamic Contact Angle in Microchannel Flows. *Journal of Bionic Engineering* 2008, 5.

[9] M. Queralt-Martín, M. Pradas, R. Rodríguez-Trujillo, M. Arundell, E. Corvera Poiré, and A. Hernández-Machado. Pinning and Avalanches in Hydrophobic Microchannels. *Phys. Rev. Lett.* 2011, 106.